Zoomorphology
DOI 10.1007/s00435-017-0371-x

ORIGINAL PAPER

Ultrastructure of the extracorporeal tube and "cement glands" in the sessile rotifer *Limnias melicerta* (Rotifera: Gnesiotrocha)

Hui Yang[1] · **Rick Hochberg**[1]

Received: 12 June 2017 / Revised: 12 June 2017 / Accepted: 24 July 2017

Abstract Rotifers are common aquatic microscopic invertebrates. Most rotifers are planktonic but several gnesiotrochan species are sessile and produce tubular sheaths around their bodies. These tubes have a variable morphology and may be produced by different glands. Here, we applied scanning electron microscopy (SEM) and transmission electron microscopy (TEM) to study the ultrastructure of the tube and its potential origin of secretion in *Limnias melicerta*. Results from SEM confirm earlier observations that juvenile rotifers first secrete a segment-less tube and then add segments as they grow. Tubes consist of two distinct secretions: an inner mucus-like layer that extends from the base to the foot region of the adult, and an external layer that is secreted by "cement cells" sensu Wright. The external layer consists of a series of thickened rings and elongated girdles, both of which are somewhat fibrous in appearance and occasionally show differences in electron density. The ultrastructure of the "cement cells" indicates that these secretory regions are not cellular but rather a modified region of the syncytial integument that forms a belt-like gland around the animal. This gland is highly papillated due to localized folding of the intracytoplasmic lamina of the integument. The ultrastructure of the gland shows a voluminous swelling of the syncytium with abundant endoplasmic reticulum and secretion vesicles. At least three types of membrane-bound secretion vesicles are present based on electron density. We hypothesize that the gland is constitutively active but secretions are only released when a threshold level is reached.

Keywords Integument · Secretion · Defense · Sessile · Plankton

Introduction

Phylum Rotifera comprises approximately 2000 species of microscopic invertebrates that are widely distributed in almost every freshwater system (Segers 2007). They are normally characterized by a ciliated region on top of the head (corona), a muscular pharynx (mastax) containing a set of hardened jaws (trophi), and a syncytial integument with an intracytoplasmic lamina (Kolisko 1939; Edmondson 1944, 1945; Wallace et al. 2006). Most rotifers are free-swimming, but species from three families—Atrochidae, Collothecidae, and Flosculariidae—are mostly sessile on submerged vegetation. Many of these rotifers produce tubular sheaths of extracellular secretions that surround their bodies and presumably functions for camouflage and/or defense (Wallace and Snell 2009). These secretive tubes can be morphologically diverse but in general fit into one of the three categories: a transparent mucus sheath as in *Collotheca campanulata* Dobie, 1849 (Wright 1959), a tube of pseudo-fecal pellets atop a gelatinous layer as in *Floscularia ringens* Linnæus, 1758 (Gosse 1851; Cubbitt 1872; Wright 1950; Fontaneto et al. 2003), and a hardened tube with a uniquely ringed pattern as in *Limnias melicerta* Weisse, 1848. Currently, there are few ultrastructural details on any of these tubes and scarce data on their possible anatomical origins, making an understanding of their evolutionary origins difficult to ascertain.

✉ Hui Yang
hui_yang@student.uml.edu

Rick Hochberg
rick_hochberg@uml.edu

[1] University of Massachusetts Lowell, One University Avenue, Lowell, MA 01854, USA

Published online: 09 August 2017

To date, the only tube-building rotifers that have been examined in any detail are *F. ringens* and *L. melicerta*. In *F. ringens*, the tube is built from pellets that appear to be a mixture of suspended particles combined with secretions from a specialized region of the rotifer's corona called the modulus (Wright 1950; Fontaneto et al. 2003). Underlying these pellets is a thin gelatinous matrix of unknown origin (Fontaneto et al. 2003). In *L. melicerta*, the anatomical source of the tube appears to be entirely different. Wright (1954) made lengthy light microscopical observations of the tube-building process in this species and revealed that "cement cells" in the trunk region appeared to exude the tube secretions. The cement cells appeared to secrete a hyaline matrix around the juvenile after settlement. This secretion took only a few minutes to produce and was followed by a period of 24–48 h before further secretions were generated. To further build the tube and thus protect the entire body, the animal would contract its foot and press a glandular portion of her trunk against the rim of the tube to force secretions from her cement cells. Each round of secretion would last several minutes and lead to the deposition of a posterior ring (thickened belt of secretion that overhangs the original edge of the tube) and a hyaline girdle that would extend some distance anteriorly (see Wright 1954). Thus, over the course of the rotifer's life, a series of rings and girdles would be produced every few days, eventually leading to the characteristic pattern common to the species' tube, thus solving "the mystery of the rings" by, as Wright (1954) opined, "the greatest good fortune".

Observations of tube secretion in rotifers are fraught with difficulties because the animals are extremely small (generally <1 mm), highly transparent, and produce their secretions fairly rapidly (in minutes). Moreover, the identification of the possible sources of the secretions (glands) is difficult because in all likelihood, the sources themselves (glands) are transparent and only a few microns in size. Here, we use Wright's (1954) "good fortune" to investigate the possible source of the extracorporeal tube in *L. melicerta*. Based on his study, we knew approximately where to look in the animal for the cement cells. We then used scanning and transmission electron microscopy to characterize the cement cells and their secretions.

Materials and methods

In the summer of 2016, we collected specimens of *L. melicerta* from Flint Pond in Tyngsboro, MA (42°40′29″ N, 71°25′34″W) and cultured them on submerged leaves of *Elodea canadensis* in an aquarium filled with native pond water at the University of Massachusetts Lowell. Rotifers were identified with brightfield and DIC microscopy on a Zeiss Axioskop A1 and photographed with a Sony digital Handycam camera.

For SEM observation, specimens were anesthetized with individual drops of 0.5% bupivacaine, fixed in 2.5% glutaraldehyde in 0.1 mol phosphate buffer (PB, pH 7.3) for 2 h, rinsed in 0.1 mol PB for 1 h, post-fixed in 1% OsO_4 in 0.1 mol PB for 1 h, and rinsed in 0.1 mol PB for 1 h. The specimens were subsequently dehydrated in an ethanol series (70, 90, 100%), and critical point dried (CPD) in a Tousimis SamDri PVT-3D (Hochberg et al. 2015). After CPD, specimens were mounted on aluminum stubs. Some tubes were carefully torn open by OOO insect pins to expose the animal. Specimens were coated with gold and viewed on a JEOL JSM 6390 SEM.

For TEM, specimens were fixed and dehydrated (without CPD) as in SEM, then placed in propylene oxide (PO) for 20 min (2×), and slowly infiltrated in a PO-epoxy resin mixture (Araldite, EMbed 812; Electron Microscopy Sciences) in ratios of 3:1, 1:1,1:3 for 1 h, respectively, and in pure resin overnight. Specimens were embedded in pure epoxy resin the next day, cured in an oven at 60 °C for 24 h, and sectioned at 70–90 nm on a Leica EM UC6 Cryo-Ultramicrotome. Sections were stained in uranyl acetate and lead citrate and examined on Phillips EM 400T electron microscope equipped with an Advantage HRL-B bottom mounted 1.3 Megapixel CCD camera and a Pentium computer at the University of Massachusetts Medical School in Worcester, MA. Digital photos were analyzed in ImageJ 1.51 h, cropped and edited for brightness and contrast in Adobe Photoshop; no further changes were made.

Results

External fine structure of the tube

Multiple tubes were examined ranging in length from 204 µm to 599 µm (average 438 µm). Tubes were normally narrower at their base (34–42 µm) and wider at the anterior end (60–67 µm). For example, an adult tube of 594 µm length with a base of 41 µm diameter would increase to 50 µm diameter in the first 100 µm and remained the same until it expanded (flared edges) at the opening. Bacteria and debris were present on most tubes examined with brightfield microscopy and SEM (Fig. 1a–d). The top opening of the tube was slightly flared out. All tubes showed an iterative pattern along their length consisting of a posterior ring (ridge-like belts between girdles) and anterior girdle (short columns). The posterior region of all tubes lacked this segmentation and was entirely smooth. The smooth portion was mostly apparent in juvenile rotifers where only

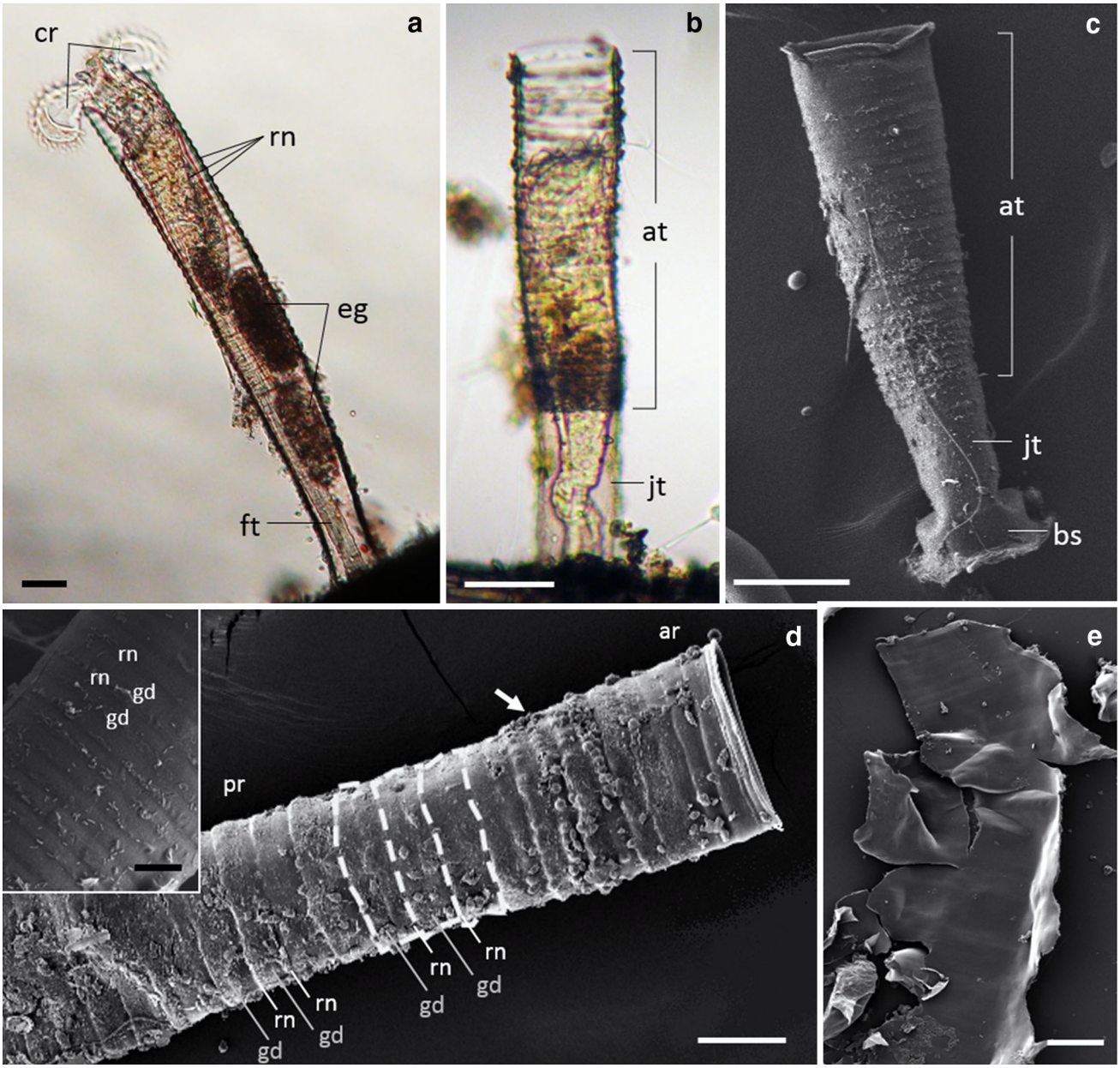

Fig. 1 Fine structure of a *L. melicerta* tube. **a** Brightfield view of an adult animal with the corona protruding from the tube. The adult tube is defined by the segmented ring (rn) pattern. **b** Brightfield view of a young adult a few days after settlement. The *ring pattern* is produced only after the juvenile portion of the tube (jt, no rings) is secreted. **c** SEM of tube of similar age to the tube in **b**. The diameter of the apical opening is slightly wider than the base. Bacteria and fine debris are present on the tube. **d** SEM of an adult tube showing the series of rings and girdles. *Dash lines* highlight the rings, while the area between the *dash lines* represents the girdles. *Arrow* microorganism and/or debris deposition. *Inset* rings and girdles of a new tube, the pattern is relatively smooth compared to the adult tube. **e** SEM of a broken tube showing the smooth interior side. *ar* anterior, *at* adult tube, *bs* base, *cr* corona, *eg* egg, *ft* foot, *gd* girdle, *jt* juvenile tube, *pr* posterior, *rn* ring. *Scale bars* **a**–**e** 50 µm, **d** *inset* 10 µm

a few segments had been produced at the anterior end and little debris was present (Fig. 1b, c). The smooth regions were featureless and 66–70 µm long in both juvenile and adult tubes. Beyond this "juvenile" section of the tube were the individual segments that begin with a thickened ring and elongate girdle (Fig. 1d). Each girdle was smooth in appearance and demarcated from subsequent girdles above and below by the exterior ring (Fig. 1d, inset). The girdles were typically 2–6 µm (average 4.5 µm) in length and were shorter at the bottom and longer towards the top. In an adult, there were a few girdles exceedingly long (about 14 µm) in the middle of the tube (Fig. 1d). The inner surface of the tube was extremely smooth with no trace of ring or girdle (Fig. 1e).

Ultrastructure of the tube

Tubes were examined in cross, oblique (ca. 45°), and longitudinal sections. We note that Wright's application of the terms "girdle" and "ring" do not appear to apply as well at the ultrastructural level as they do for brightfield microscopy and SEM. Nevertheless, we use this terminology to maintain consistency with his original description. All tubes consisted of two layers of material with different electron densities (Fig. 2a–c). The most internal layer (towards the animal) was an evenly distributed mucus-like secretion ca. 1.25 μm thick. The layer was mostly homogeneous in appearance though the inner edge of the mucus was slightly more electron dense than the rest of the matrix (Fig. 2c). We also note that the mucus did not extend the length of the tube but was restricted to the juvenile and adult foot region; precisely where the mucus layer stopped was not determined. The second or external layer of the tube was more electron dense than the mucus layer—this was characteristic of both the adult portion of the tube in the foot region (Fig. 2a–d) and the juvenile portion of the tube (Fig. 2e). The segmented region of the adult tube was also thicker than the mucus layer: rings were 3–6 μm thick and girdles were 2–3 μm thick. In some regions, layer 2 showed differences in electron density between its inner and external sides. The inner side was often more electron dense than the external side, which often appeared fibrous (Fig. 2b, c). However, these differences in electron density were not consistent along the length of the tube.

Sections through the tubes showed a very thin lamina (Fig. 2c, i, arrow) bisecting layer 2 at an oblique angle. This angled lamina differentiates each round of secretion, i.e., each individual segment consisting of a ring and girdle was separated from anterior and posterior segments by this lamina. Longitudinal sections revealed that each segment of the adult tube is laid down at an oblique angle (Fig. 2f–i), with a sharp, elongate posterior portion (12.5 ± 0.97 μm) along the inner wall (not visible from the external surface via LM or SEM), a hump-like thickening (Wright's ring) at the approximate center (Fig. 2i, outlined), and an anterior region that is short and rounded (Wright's girdle).

Fine structure of the integument

The integument was smooth when viewed with bright field microscopy and at low magnification SEM (Fig. 3a). At higher magnification SEM, the morphology of the integument was highly diverse; some regions were smooth while others were heavily papillated and/or wrinkled (Fig. 3b). The coronae of all specimens were retracted, revealing a smooth integument that covered the retracted region (operculum sensu Wright 1954). This region generally faces the opening of the tube when an animal's corona is retracted. Seven nodules protruded from the operculum in the following pattern: two ventral, three medial, and two dorsal (Fig. 3b, inset). Several of the nodules in each row were interconnected by a thin fold in the smooth integument. Posterior of the operculum on the dorsal side was a papillated region that extended back to the cloacal opening (Fig. 3b, c). This papillated region extended all the way around the animal's perimeter in a belt-like fashion. The papillae did not extend on to the paired antennae on the ventral side (Fig. 3b, e). All individual papillae were extremely small and could not be accurately measured with SEM (Fig. 3d). On each lateral side was a triangular area with very dense ridges or folds that extended diagonally (Fig. 3e outlined); this pattern might be the result of the retracted corona. The remainder of the integument in the trunk region was relatively smooth with very fine ridges dispersed between folds in the body wall.

TEM revealed that the body wall was sparsely covered with glycocalyx. The integument of the trunk region (corona not observed) was syncytial and composed of two main layers: an apical, electron-dense intracytoplasmic lamina (ICL, layer 1) and a basal, electron-lucent region (layer 2) containing many organelles (Fig. 4). Apically, the syncytium was covered by a single plasma membrane that had a wavy appearance (18.3 ± 3.4 nm, Fig. 4a). The ICL beneath was amorphous in appearance and had a thickness of 47–235 nm (average 130 ± 42.5 nm) depending on whether the integument was flat, papillated or folded. The papillated region was composed solely of ICL and 98 ± 27 nm thick (Fig. 4a–c). The grooves and ridges in the lateral regions of the anterior trunk were folds of layers 1 and 2 that extended up to 900 nm in height (Fig. 4b, c). Layer 2 varied in thickness across the trunk from regions where it was nearly indistinguishable to areas where it reached 4.7 μm thick (gland areas, Figs. 4d–f, 5). Beneath layer 2, there was a thin basal lamina (54 ± 15 nm) that

Fig. 2 Ultrastructure of a *L. melicerta* tube. **a** Cross section of the tube near the foot showing a portion of the animal (an) and an egg (eg) inside the tube space. **b** A higher magnification showing the inner mucus layer (L1), the outer hardened layer (L2), and a portion (foot and muscles) of the animal (an). **c** Higher magnification showing the mucus layer with even electron density and external layer with a fibrous character. *Arrow* there is also a division lamina between adjacent tube segments. **d** Portion of the tube wall towards its base showing a region of higher L1 thickness. **e** Section of the juvenile portion of the tube. **f** Section of the tube and a portion of the adult animal near the gland region. **g**, **h** Section near the corona. **i** Section through a tube segment. **j** Same region as I but with the entire secretion (*ring* and *girdle*) outlined. *an* animal, *ar* anterior, *at* adult tube, *ci* cilia, *cp* concealed portion of the segment *eg* egg, *ex* exterior, *gd* girdle, *in* interior, *jt* juvenile tube, *pr* posterior, *rn* ring, *sp* space. *Scale bars* **a** 10 μm, **b**, **e**, **h**, **i**, **j** 2 μm, **c** 1 μm, **d**, **f**, **g** 5 μm

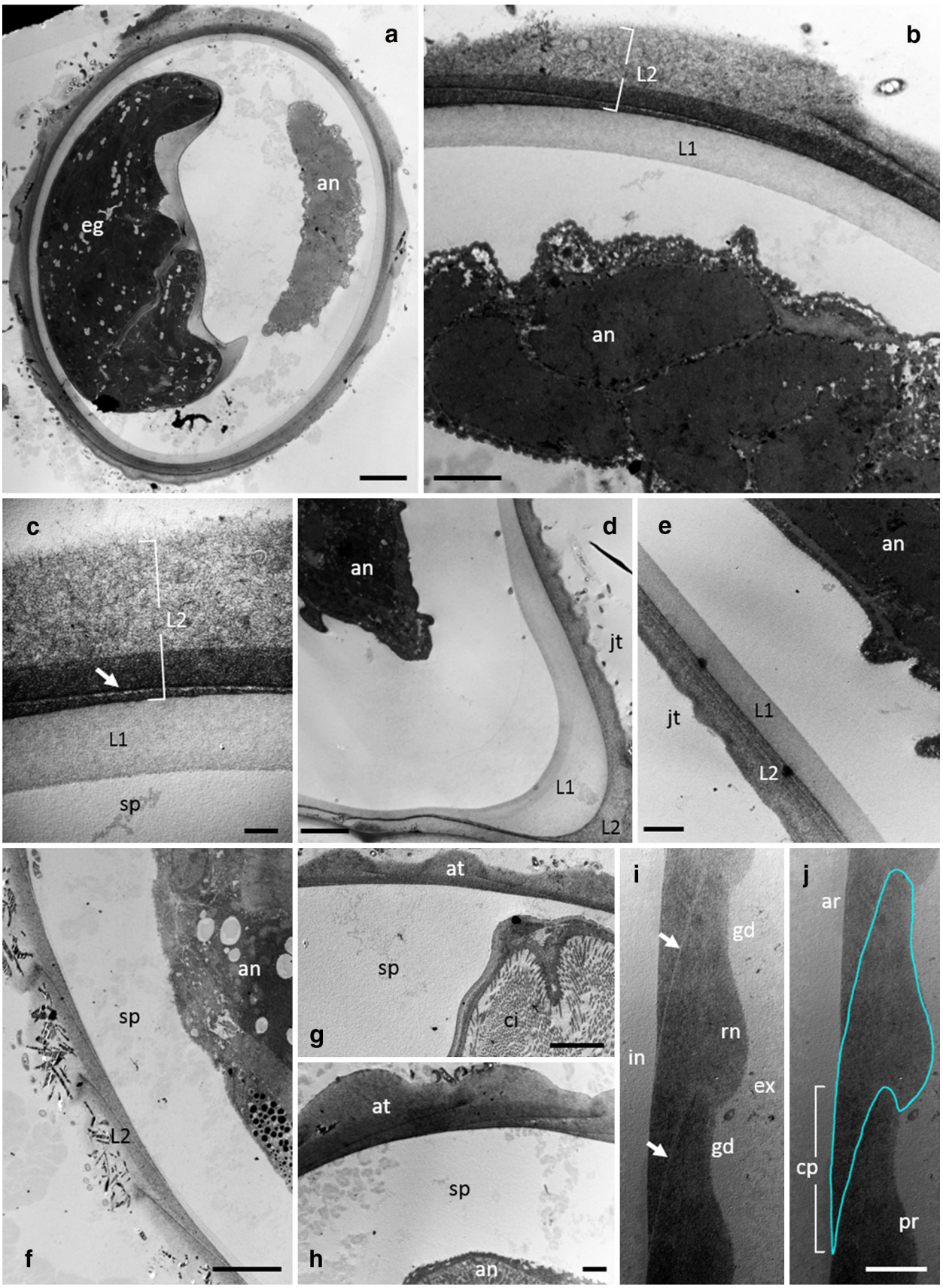
a
an
eg
b
L2
L1
an
c
L2
L1
sp
d
an
jt
L1
L2
e
an
jt
L1
L2
f
an
sp
L2
g
at
sp
ci
h
at
sp
an
i
gd
rn
in
ex
gd
j
ar
cp
pr

separated the integument from the internal organs and body cavity.

A highly glandular region of integument was present in the anterior trunk in the same approximate position as Wright's (1954) cement cells (Fig. 5). This region was in continuity with the syncytial integument of the anterior trunk, i.e., there were no detectable plasma membrane that separated the glandular region from the rest of the integument, either anteriorly where the gland was thin or posteriorly where it was significantly swollen (Fig. 5d). The integument in the anterior region gradually changed from thin and identical to the non-glandular integument (just posterior of the corona) to one showing evidence of increasing secretion vesicles and increasing thickness (as sections were taken more posteriorly). In fact, the main glandular region was much thicker (4.7 ± 0.7 µm) than the integument in any other region of the body (compare Figs. 4 and 5). The thickness was mostly due to an increase in the volume of layer 2, which was heavily populated with rough endoplasmic reticulum, mitochondria, numerous membrane-bound secretory vesicles, and Golgi apparatus. There were at least three types of membrane-bound secretion vesicles in layer 2 based on electron density (Figs. 4d–f, 5): darkly stained (t1), intermediately (gray) stained (t2) and electron-lucent vesicles (t3). The electron-dense vesicles (diameter = 340 ± 44.5 nm) had a bounding membrane that could be distinguished from the internal secretion that often had a patchy appearance (Fig. 5b, c). The e-dense secretions were more abundant in the basal region of layer 2 compared to the apical region nearest the ICL (Fig. 5d, e); no sections revealed exocytosis of these e-dense secretions. The intermediately stained (360 ± 119.9 nm) and electron-lucent vesicles (width = 210 ± 48.6 nm, length = 230 ± 41.3 nm) also had a distinguishable membrane but the contents were difficult to visualize. There were also numerous smaller vase-shaped vesicles connecting layer 2 and the ICL; these vesicles formed a neck through the ICL (Fig. 5, arrows). Rough endoplasmic reticulum was most abundant in the basal region of layer 2, but was also dispersed between secretory granules towards the apical region as well. Free ribosomes were present throughout the glandular region (Figs. 4, 5). Golgi stacks were present mostly in the flattened region of the gland (Fig. 5f). Nuclei were noted around the integument but not within the body of the glands themselves, but this might be an artifact of the lack of serial sections. The glandular region was bound basally by a thin basal lamina that contacted longitudinal muscle or gut tissue.

Discussion

Since Antony van Leeuwenhoek's first description of rotifers in 1674 (Ford 1982), and their more formal recognition by Carolus Linnaeus in 1758, the morphological diversity of rotifers has impressed biologists, microscopists, and photographers alike. In one lineage, however—the Gnesiotrocha—their diversity extends beyond animal morphology into what may be considered an extended phenotype (sensu Dawkins 2016), which in the case of many sessile and some planktonic rotifers are the secretory tubes that surround, camouflage, and/or protect their bodies. Among the variety of tube morphologies known within the Gnesiotrocha (Fontaneto and De Smet 2015; Wallace et al. 2015), the type produced by *Limnias melicerta* is exceptional. The hyaline tube bears regular segments along its length and is unlike any other secretion in the Rotifera, prompting many early scientists to wonder how such iterative patterns were formed (Cubbitt 1871; Rousselet 1889). However, the small size of the animals and their "flagging interest" in building the tube (it could take 24–48 h to deposit even a small segment of tube) have prevented proper descriptions of the process (Wright 1954). But, with good fortune and more importantly, a great amount of patience, Wright (1954) witnessed the moment when an adult *L. melicerta* deposited a series of secretions onto its existing tube, thus revealing how the segment-like patterns were made. His observations provided the first insights into the secretory processes of tube building in sessile rotifers, but a lack of follow-up studies on tube morphology or tube-building behavior have prevented a more clear and detailed understanding of the process. To date, observations of tube morphology and tube building have been limited to light microscopical (Wright 1950, 1954) and occasionally scanning electron microscopical observations (Fontaneto et al. 2003), but have yet to examine the tubes or the glands that produce them at an ultrastructural level. In this study, we utilized both scanning and transmission electron microscopy to further explore the morphology of the rotifer, the secreted tube, and the anatomical origin of the secretion.

Wright described the tube of *L. melicerta* as essentially a stack of circular segments, each consisting of a posterior ring (belt) and an anterior girdle that are deposited simultaneously every few days, eventually leading to the segmented pattern characteristic of the adult tube. Interestingly, when the tube is first secreted, there are no segments, but only a smooth and featureless hardened tube

Fig. 3 External ultrastructure of *L. melicerta* integument. **a** SEM of the animal at low magnification showing the whole body except the base of the foot. **b** Anterior trunk of the animal, showing the papillae and wrinkles around the neck, and the cloacal opening at the dorsal side. *Inset* frontal view of the operculum showing the nodules. **c** Cloacal opening and the dorsal area just below the neck. **d** Papillae at higher magnification. **e** Ventrolateral view of the animal, showing a triangular area of dense ridges and folds. *co* cloacal opening, *ft* foot, *op* operculum, *pa* papillated area, *tk* trunk *va* ventral antennae. *Scale bars* **a** 50 µm, **b**, **c**, **e** 10 µm, **d** 2 µm

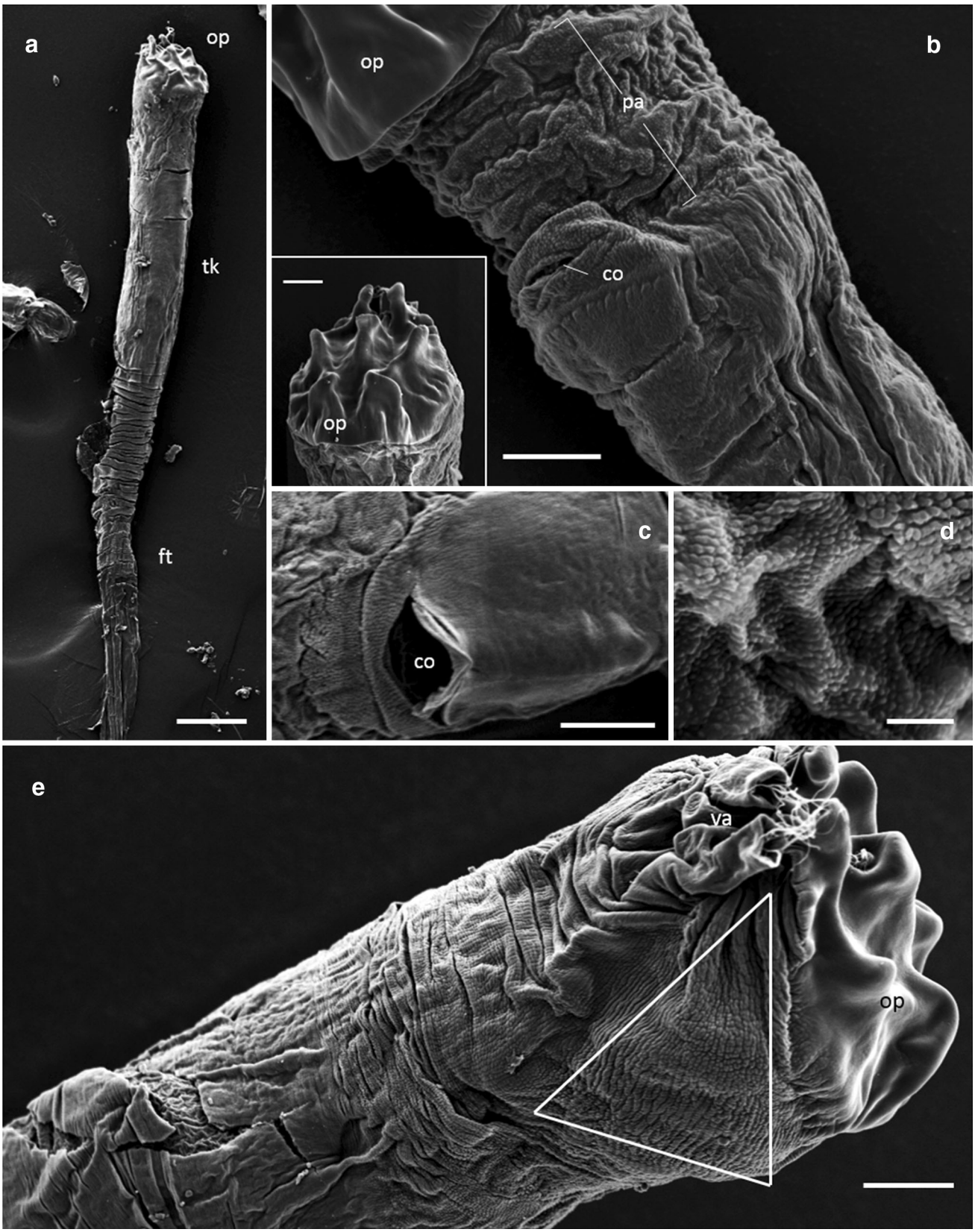
a
op
tk
ft
b
op
pa
co
op
c
co
d
e
va
op

(theca of Wright 1954) that is approximately the same length as the juvenile. This juvenile tube is apparently secreted by the same glands and in a similar fashion to the adult tube that is produced on top of it (Wright 1954). Wright described the tube as consisting of a singular hardened secretion, but interestingly, our TEM results revealed that there is a second layer hidden on the inside of this juvenile tube—an electron-lucent mucus-like layer to 1.25 µm thick—that Wright never observed. This inner layer is homogeneous in ultrastructure and appears to be present in the juvenile portion of the tube and at least part of the foot region of the adult tube—the exact length of this region could not be determined. The origin of this mucoid layer is unknown since neither Wright's observations nor our own could verify when it was secreted (before or after the hardened matrix) and from where. Its mucoid-like appearance and dissimilar ultrastructure from the hardened matrix suggests it has a different origin from the segmented tube.

Only after the juvenile tube is produced are the iterative secretions that constitute the rings and girdles secreted over the life of the animal. Wright (1954) showed that each iteration begins with the rotifer contracting posteriorly, thus bringing its cement cells into contact with the rim (opening) of the existing tube and causing the secretions to flow from the cells onto the hardened juvenile tube. The animal would then extend anteriorly as the exudates flowed from the cells, thus extending the length of the tube anteriorly. As a result, each round of secretion begins with a newly deposited thickened ring (due to posterior compression by the cells) followed by a thinner hyaline girdle that is drawn upward and flared outward at its anterior edge (the new tube opening). However, this description is not complete because during the compression stage to make the ring, some exudate appears to flow along the inner margin of the tube and line the previous girdle (Wright 1954: Fig. 4). Consequently, each round of secretion actually consists from posterior to anterior of a concealed exudate inside the previous girdle, the newly deposited ring, and then the newly deposited girdle. Subsequent rounds of secretion follow this pattern. Our TEM results revealed that the concealed exudate lines the inside of the tube to approximately the previous ring (on its inner surface), and can be distinguished from it by a thin lamina of different electron density (Fig. 2i). This internal exudate may be what binds the new segment to the older segment and stabilizes the tube along its length. Thus, any future studies that want to measure secretion in this animal and relate it to growth of the tube must take into account that each segment is more than the sum of the ring and girdle as viewed from the outside of the tube.

We note that tube ultrastructure has a mostly homogeneous appearance along its length with a smooth inner wall and a somewhat fibrous external surface. This is consistent across specimens, but we also noticed that in some tubes there was a distinct difference in electron density in some regions of individual tubes. For example, some segments had an inner exudate that was more electron dense than the external ring and girdle on top of it (Fig. 2b). We are uncertain of the reason for these differences, but hypothesize that it might be related to the age of the segment. While we did not keep track of when segments were produced, we think it is possible that newer (younger) segments may be those that show the more electron dense secretions, while older segments have matrices that are largely identical in electron density throughout. This would suggest that the chemistry of the secretions changes over time perhaps as the matrix hardens.

As mentioned, the tube of *L. melicerta* consists of two different secretions, with Wright (1954) hypothesizing that the hardened matrix (tube layer 2 of this study) was produced by "cement cells." Wright's hypothesis was based on extensive behavioral observations, but he never made any further inquiries into the histology of these cells. Our observations with SEM revealed this region with the cement cells to have a highly papillated surface, at least some of which covers the glandular area that we hypothesize corresponds to Wright's "cement cells." With TEM, we revealed that the papillated region, and in fact other portions of the integument, are similar to the integument of other monogononts (e.g., Koehler 1965, 1966; Clément 1969, 1980; Storch and Welsch 1969; Brodie 1970; Schramm 1978; Hendelberg et al. 1979; Clément and Wurdak 1991; Hochberg et al. 2015, 2017), which is syncytial and consists of an apical intracytoplasmic lamina (ICL, layer 1) and a basal electron-lucent cytoplasm (layer 2). In *L. melicerta*, the thickened ICL matrix of the papillated region and non-papillated regions (the remaining trunk) is mostly amorphous while in other gnesiotrochans such as *Sinantherina socialis* (Hochberg et al. 2015) and *Cupelopagis vorax* (Hochberg et al. 2017) it may be amorphous, finely granular, or fibrous (depending on the region). Layer 2 is also similar between *L. melicerta* and

Fig. 4 Ultrastructure of *L. melicerta* trunk integument and the glandular region. **a** TEM of the integument in the triangular area of Fig. 3e, showing a syncytial construction with two main layers. The intracytoplasmic lamina (*L1*) is thin and forms small mounds on the surface. The organelle-containing portion of the integument (*L2*) is thick and bordered basally by a basal lamina. **b** Integument at the papillated region showing grooves and ridges formed by both layers and small mounds/papillae formed by *L1*. **c** Higher magnification of the grooves and ridges. **d–f** *L2* region showing significant swelling near the trunk gland and containing a large amount of endoplasmic reticulum (ER) and vesicles. *Arrow* mitochondria. *bl* basal lamina, *gg* Golgi apparatus, *gv* groove, *md* mound, *rg* ridge, *t1–t3* type 1–3 vesicles. *Scale bars* **a**, **b**, **f** 0.5 µm, **c**, **d** 2 µm, **e** 1 µm

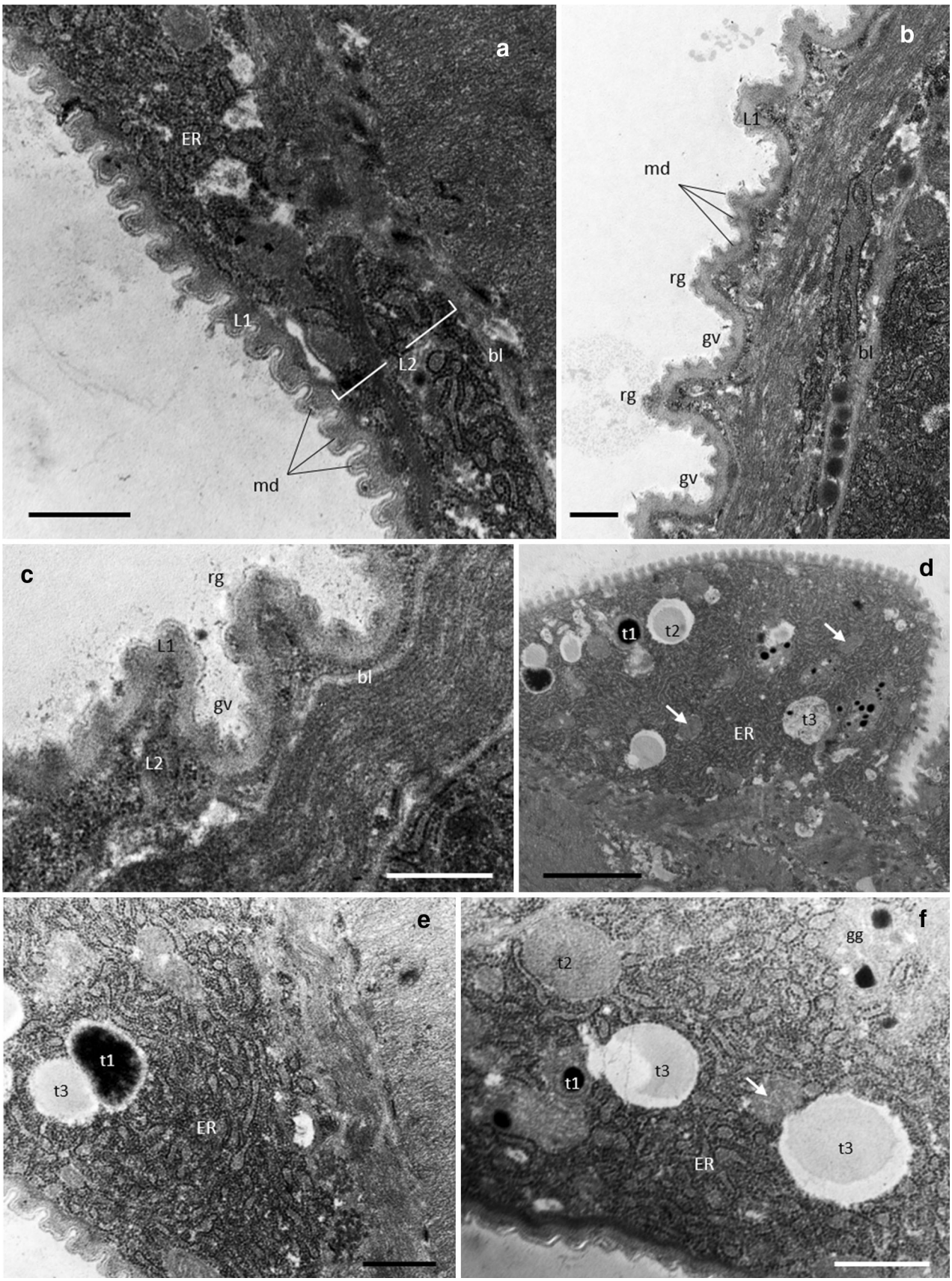
a
ER
L1
L2
bl
md
b
L1
md
rg
gv
bl
rg
gv
c
rg
L1
bl
gv
L2
d
t1
t2
t3
ER
e
t1
t3
ER
f
gg
t2
t1
t3
t3
ER

other gnesiotrochans; however, a notable difference occurs in the region of the cement cells. The electron-lucent cytoplasm gradually fills with large membrane-bound secretions as the layer also increases in thickness from anterior to posterior. Eventually, this layer becomes extremely swollen and forms an almost complete belt around the perimeter of the animal. Our cross sections were not perfectly perpendicular to the long axis of the animals; so we are uncertain if the gland truly extends around the entire perimeter. With SEM, it is difficult to discern precisely where this belt is since the glands do not produce an obviously swollen region like they do in the defensive warts of *S. socialis* (Hochberg et al. 2015). The glandular region of *L. melicerta* is clearly beneath a portion of the papillated integument, but without longitudinal sections to show the position of the gland relative to the corona or another externally distinguishable region, it remains unknown precisely where it is.

The glandular region contains at least three types of membrane-bound secretion vesicles based on electron density, and there were several areas where these vesicles appeared to be in continuity with each other and/or produced in a singular area (Fig. 4c–e). Regardless, vesicles were always surrounded by a very extensive rough endoplasmic reticulum, but curiously, our sections revealed surprisingly little Golgi, though this is likely an artifact of incomplete serial sections. Several of the smaller electron-lucent vesicles appeared to be fused with the overlying ICL (Fig. 5), perhaps to release their contents, but this was never observed for the more electron-dense secretions. However, if these secretions are those that form the hardened tube, then we would not expect to see evidence of exocytosis except for only during times of tube-building (more below). Importantly, none of our sections ever revealed a plasma membrane delimiting the glandular region from the remaining integument, suggesting that the gland is not in fact cellular as originally described by Wright (1954). Instead, the gland appears to be just a highly localized cytoplasmic region of secretory activity, though the secretion vesicles do spread out across the cytoplasm in some areas and away from their sites of origin (based on the lack of rough ER and Golgi).

While we were never able to witness the secretory process of *L. melicerta*, we nevertheless have an idea about how the process might work based on Wright's (1954) observations and our own SEM and TEM observations. We hypothesize that the gland is probably constitutively active and may have to reach some critical level of secretion accumulation before the animal can release the contents. Exocytosis is then probably a voluntary process that requires compression of the gland against the preexisting tube to force the membrane-bound vacuoles to merge with the ICL and exocytose their products. This differs from the exocytosis of smaller vesicles that is normally observed in the rotifer integument (see Clément and Wurdak 1991 and references therein; also Hochberg et al. 2015, 2017). The contents of these smaller vesicles may be components of glycocalyx since they are present in all species and are independent of tube-building behavior. Curiously, we have never witnessed pores in the integument of any rotifer using SEM, which would be expected for animals that generate as many secretions as they apparently do. However, such pores would be exceedingly small (few nanometers) and beyond the limits of SEM resolution; still, perhaps such pores would be measurable in *L. melicerta* if caught during the act of tube secretion, considering that the membrane-bound vesicles are much larger, more numerous, and might in fact merge during exocytosis. We note that some vesicles of different staining qualities do appear to fuse prior to exocytosis (Figs. 4, 5). The presence of at least three types of secretory vacuoles (based on electron density) further suggests that the tubes may be made of different compounds (e.g., proteins, glycoproteins, minerals), but this is purely speculative and would require special staining or extraction techniques to verify the contents of individual vesicles.

Altogether, our observations reveal that the cement cells of *L. melicerta* represent a highly unusual form of exocrine gland (singular) in the Rotifera. This gland appears to be a highly specialized and regionalized zone of the syncytial integument that lacks ducts or pores (e.g., as in acinar glands) and whose secretion requires voluntary activities by the host to exocytose the products. While these observations provide some important insights into tube secretion, we still lack basic information that is necessary to fully understand the underlying process of secretion such as: the origins of the inner mucus layer in the juvenile tube; how the hardened matrix of the juvenile tube is secreted in the absence of a tube against which to compress the glands (but see Wright 1954 for a hypothesis); the chemistry of the different vesicle types in the glands; the chemical composition of the tubes themselves (and if they differ based on the chemistry of the surrounding waters); and what

Fig. 5 Ultrastructure of the glandular region (cement cells) near the neck. **a** Cross section of the gland integument showing a thickened cytoplasmic layer (*L2*) and large number of vesicles. **b** Higher magnification of the apical gland integument. **c** Basal section of the gland integument. **d** Transection of the gland region, showing more vesicles at anterior (*left*) and more ER at the posterior (*right*). **e** Higher magnification of the vesicles. The electron dense secretions are more concentrated in L2 with no evidence of exocytosis. *Arrow* electron-lucent vesicles are more abundant near *L1* and some of them are fused with *L1*. **f** Section through a gland showing a variety of secretion organelles. *bl* basal lamina, *ER* endoplasmic reticulum, *gg* Golgi apparatus, *L1* intracytoplasmic lamina, *t1, t2* secretion vesicles. *Scale bars* **a**, **d** 2 μm, **b**, **c** 0.2 μm, **e** 1 μm, **f** 0.5 μm

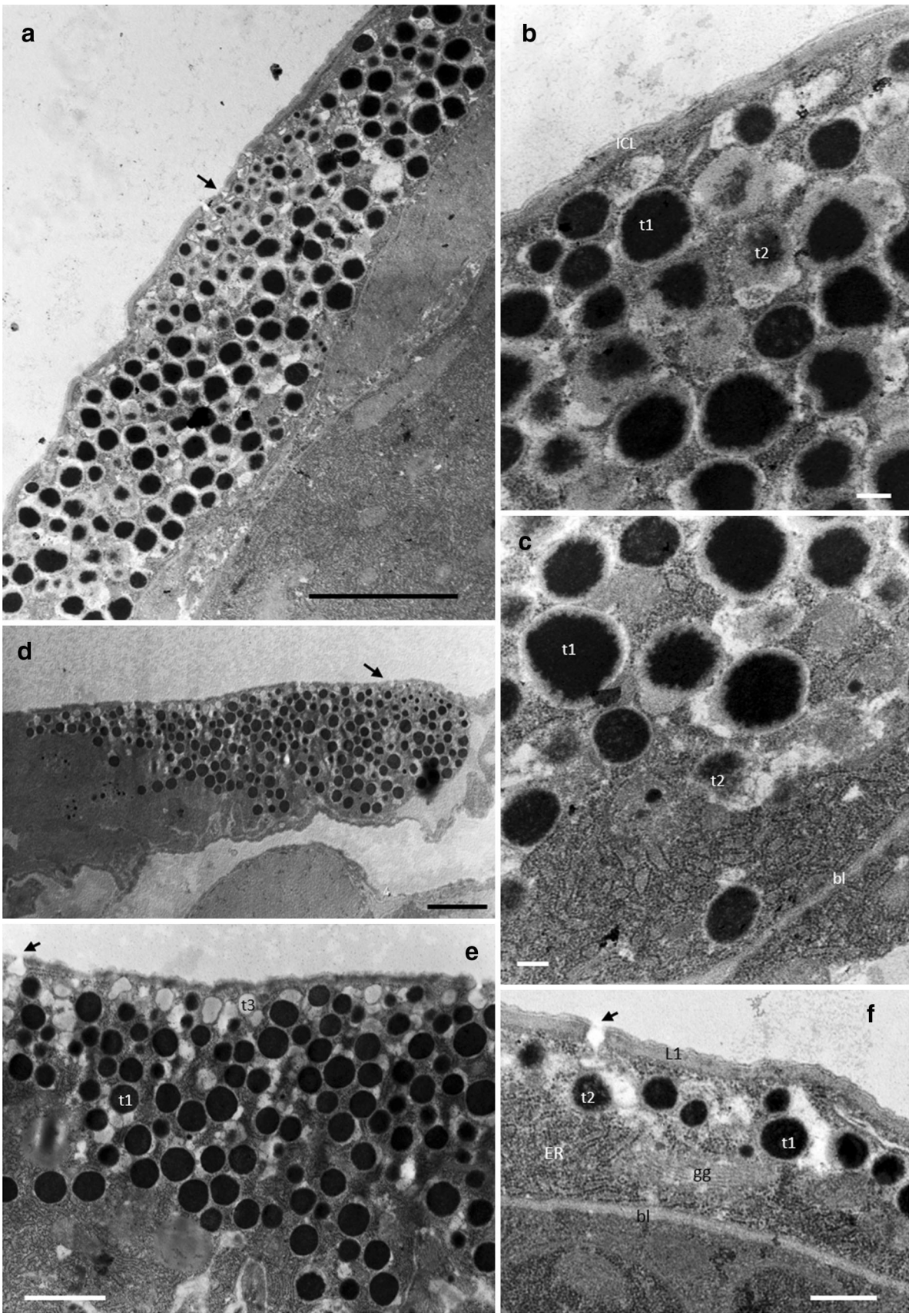
a
b
ICL
t1
t2
c
t1
t2
bl
d
e
t3
t1
f
L1
t2
t1
ER
gg
bl

determines the periodicity of the secretion process (is it determined by the animal or does the animal respond to vesicle accumulation in the glands?). We think that further behavioral and ultrastructural studies of *L. melicerta* may provide the missing information that can better explain this unique process and offer additional insights into the evolution of tube production in this exceptional rotifer.

Acknowledgements The authors acknowledge funding by the National Science Foundation to support this research (DEB 0918499 to R. Hochberg).

Compliance with ethical standards

Conflict of interest The authors declare that they have no conflict of interest.

Funding This study was funded by National Science Foundation (Grant number DEB 0918499 to R. Hochberg).

Research involving human participants and/or animals This article does not contain any studies with human participants performed by any of the authors.

Ethical approval All applicable international, national, and/or institutional guidelines for the care and use of animals were followed.

References

Brodie AE (1970) Development of the cuticle in the rotifer *Asplanchna brightwellii*. Z Zellforsch Mikrosk Anat\ 105:512–515

Clément P (1969) Premières observations sur l'ultrastructure comparèe des tèguments de Rotifère. Vie Milieu 20:461–482

Clément P (1980) Phylogenetic relationship of rotifers, as derived from photoreceptor morphology and other ultrastructural analyses. Hydrobiologia 73:93–117

Clément P, Wurdak E (1991) Rotifera. In: Harrison FW, Ruppert EE (eds) Microscopic anatomy of invertebrates, volume 4, Aschelminthes. Wiley-Liss Inc, New York, pp 219–297

Cubbitt C (1871) A rare melicertian. Mon Micr J 6:167–169

Cubbitt C (1872) Remarks on the homological position of the members constituting the thecated section of the Rotatoria. Mon Micr 8:5–12

Dawkins R (2016) The extended phenotype: the long reach of the gene. Oxford University Press, Oxford

Edmondson WT (1944) Ecological studies of sessile Rotatoria: Part I. Factors affecting distribution. Ecol Monogr 14(1):31–66

Edmondson WT (1945) Ecological studies of sessile Rotatoria, Part II: Dynamics of populations and social structures. Ecol Monogr 15(2):141–172

Fontaneto D, De Smet W (2015) Rotifera. In: Schmidt-Rhaesa A (ed) Gastrotricha, Cycloneuralia and Gnathifera. Volume 3: Gastrotricha and Gnathifera. De Gruyter, Berlin, pp 217–300

Fontaneto D, Melone G, Wallace RL (2003) Morphology of *Floscularia ringens* (Rotifera, Monogononta) from egg to adult. Invertebr Biol 122:231–240

Ford BJ (1982) The Rotifera of Antony van Leeuwoenhoek. J Quekett Microsc Club 34:362–373

Gosse PH (1851) Architectural instincts of *Melicerta ringens*. Trans Min 3:58–64

Hendelberg M, Morling G, Pejler B (1979) The ultrastructure of the lorica of the rotifer *Keratella serrulata* (Ehrbg). Zoon 7:49–54

Hochberg R, Hochberg A, Chan C (2015) Ultrastructure of the rotifer integument: peculiarities of *Sinantherina socialis* (Monogononta: Gnesiotrocha). Invertebr Biol 134:181–188

Hochberg R, Yang H, Moore J (2017) The ultrastructure of escape organs: setose arms and cross-striated muscle in *Hexarthra mira* (Rotifera: Gnesiotrocha: Flosculariaceae). Zoomorphology. doi:10.1007/s00435-016-0339-2

Koehler JK (1965) A fine structure study of the rotifer integument. J Ultrastruct Res 12:113–134

Koehler JK (1966) Some comparative fine structure relationships of the rotifer integument. J Exp Zool 161:231–243

Kolisko A (1939) Über *Conochilus unicornis* und seine Koloniebildung. Internationale Revue der gesamten Hydrobiologie und Hydrographie 39(1–2):78–98

Rousselet CF (1889) Note on a New Rotifer, *Limnias cornuella*. J Quek Micr Club Ser 2 3:337 (**pl. 4, figs. 11–14**)

Schramm U (1978) Studies of the ultrastructure of the integument of the rotifer *Habrotrocha rosa* Donner (Aschelminthes). Cell Tissue Res 189:167–177

Segers H (2007) Annotated checklist of the rotifers (Phylum Rotifera), with notes on nomenclature, taxonomy and distribution. Zootaxa 1564:1–104. In: Zootaxa. Magnolia Press, Auckland

Storch V, Welsch U (1969) Über den Aufbau des Rotatorientegumentes. Z Zellforsch Mikrosk Anat 95:405–414

Wallace RL, Snell TW (2009) Rotifera. Ecology and classification of North American freshwater invertebrates, 3rd edn, by Thorp JH, Covich AP, pp 173–235

Wallace RL, Snell TW, Ricci C, Nogrady T (2006) Rotifera Volume 1: Biology, ecology and systematics, 2nd edn. Backhuys Publishers, Leiden, The Netherlands, Knobi Productions, Ghent, Belgium

Wallace RL, Snell TW, Smith HA (2015) Phylum Rotifera. In: Thorp J, Rogers DC (eds) Ecology and general biology: Thorp and Covich's freshwater invertebrates. Academic Press, New York, pp 225–271

Wright HGS (1950) A contribution to the study of *Floscularia ringens*. J Queckett Microsc Club 4(3):103–116

Wright HGS (1954) The ringed tube of *Limnias melicerta* Weisse. Microscopy 10:13–19

Wright HGS (1959) Development of the peduncle in a sessile rotifer. J Queckett Microsc Club 4(5):231–234